Supporting Information

VolatilizableTemplates-Assisted Scalable Preparation of Honeycomb-like Porous Carbons for Efficient Oxygen Electroreduction

Wenhan Niu,[a] Ligui Li,[*,a,b] Nan Wang,[a] Shuaibo Zeng,[a] Ji Liu,[a] Dengke Zhao,[a] and Shaowei Chen[*,a,c]

[a]New Energy Research Institute, College of Environment and Energy, South China University of Technology, Guangzhou 510006, China

E-mail: esguili@scut.edu.cn

[b] Guangdong Provincial Key Laboratory of Atmospheric Environment and Pollution Control, College of Environment and Energy, South China University of Technology, Guangzhou 510006, China

[c]Department of Chemistry and Biochemistry, University of California, 1156 High Street, Santa Cruz, California 95064, USA

Email: Shaowei@ucsc.edu

Table S1. Summary of elemental concentrations in the carbon samples

Samples	XPS (at.%)							
	C	N	Fe	Cl	O	Pyridinic-N	Pyrrolic-N	Graphitic-N
PPyNSs	62.4	25.6	0.56	0.98	10.46	_	_	_
HPC-700	73.48	20.4	0.28	-	5.84	3.91	2.68	13.81
HPC-800	82.89	11.54	0.26	-	5.31	1.51	0.46	9.57
HPC-900	85.86	7.21	0.23	-	6.7	0.70	0.041	6.47
PC(NF)-800	84.11	5.39	-	-	10.5	1.74	0.23	3.42
PC(Sp/Sh)-800	87.5	6.2	-	-	6.3	1.92	0.29	3.99

Table S2. Summary of the ORR catalytic activities of heteroatom-doped carbon catalysts in 0.1 M KOH (electrode rotating speed 1600 rpm).

Catalyst	Catalyst loading (mg cm^{-2})	Half-wave potential (V vs. RHE)	Current density at 0.8 V (mA cm^{-2})	Reference
Vertically aligned N-doped CNTs	unknown	0.84	2.65	Science 2009, 323, 760
Vertically aligned N,B-codoped CNTs	unknown	0.75	1.80	Angew. Chem. Int. Ed. 2011, 50 (49), 11756
N-doped C/CNTs	0.6	0.82	3.40	Angew. Chem. Int. Ed. 2014, 126 (16), 4186
Carbon nitride/graphene	0.071	0.69	0.75	Angew. Chem. Int. Ed. 2011, 50, 5339
N-doped porous graphene	0.037	0.71	1.15	Adv. Funct. Mater. 2012, 22, 3634-3640
N,B co-doped graphene	0.28	0.69	1.00	Angew. Chem. Int. Ed. 2013, 52, 3110
N-doped graphene quantum dots	0.28	0.65	<0.2	J. Am. Chem. Soc. 2012, 134, 15
N-doped carbon nanosheets	0.60	0.84	3.20	Angew. Chem. Int. Ed. 2014, 53, 1570.
N-doped carbon nanocages	0.10	0.71	0.5	Adv. Mater. 2012, 24, 5593
N-doped ordered mesoporous carbon	0.026	0.69	0.7	Angew. Chem. Int. Ed. 2010, 49, 2565
P-doped ordered mesoporous carbons	unknown	0.67	1.7	J. Am. Chem. Soc. 2012, 134, 16127
N-doped mesoporous carbon	0.81	0.82	2.8	J. Am. Chem. Soc. 2010, 133, 206
PDA-based carbon SMSs	0.25	0.76	<2.0	Adv. Mater. 2013, 25, 998–1003
Macroporous C_3N_4/C	0.085	0.67	0.4	Angew. Chem. Int. Ed. 2012, 51, 3892
BP-NFe	0.39	0.81	<3.0	Adv. Mater. 2013, 25, 6879–6883
Meso/micro-PoPD	0.1	0.85	4.32	Nat. Commun. 2014, 5, 4973
HPC-800	**0.4**	**0.85**	**4.83**	**This work**
Pt/C	**0.2**	**0.81**	**3.00**	**This work**

Table S3. Summary of the performance of Zn-Air batteries reported in recent literature.

ORR Catalyst	Zn electrode	Electrolyte	Voltage @ 1 mA cm^{-2}	Voltage @ 10 mA cm^{-2}	Voltage @ 100 mA cm^{-2}	Reference
PEDOT	Zn rod	1 M KOH	1.07	-		Science 2008, 321, 671
CoO/N-CNT	Zn foil	6 M KOH	-	1.3		Nat. Commun. 2013, 4, 1805
FePc-Py-CNT	Zn powder	6 M KOH	1.32	1.25		Nat. Commun. 2014, 2076
Mn_3O_4/graphene	Zn powder	unknown	-	1.23	0.92	Energy Environ. Sci. 2011, 4, 4148
Amorphous MnO_x/C	Zn powder	6 M KOH	-	1.24	1.04	Nano Lett. 2011, 11, 5362
N-doped CNTs	Zn plate	6 M KOH	-	1.22	0.76	Electrochim. Acta 2011, 56 (14), 5080-5084.
Fe, Co, N-doped C	Zn plate	6 M KOH	-	-	1.1	J. Power Sources 2011, 196 (7), 3673-3677.
N-CNF aerogel	Zn foil	6 M KOH	1.34	1.25	-	Nano energy 2015(11),366-376
Meso/micro-P*o*PD	Zn foil	6 M KOH	1.36	1.28	1.01	Nat. Commun. 2014, 5, 4973
HPC-800	**Zn foil**	**6 M KOH**	**1.40**	**1.29**	**0.94**	**This work**
Pt/C	**Zn foil**	**6 M KOH**	**1.38**	**1.28**	**0.89**	**This work**

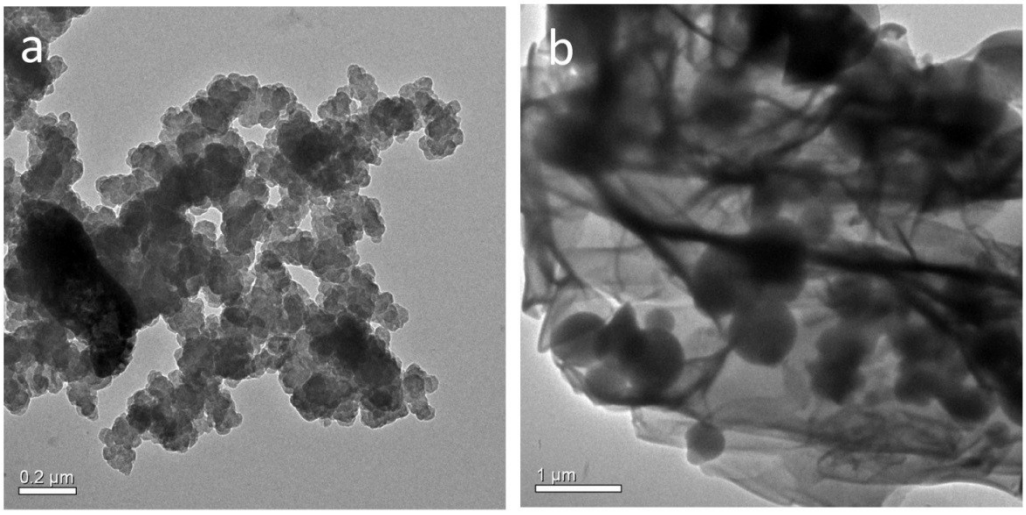

Fig.S1 Representative TEM images of (a) PPyNFs and (b)PPySp/Sh.

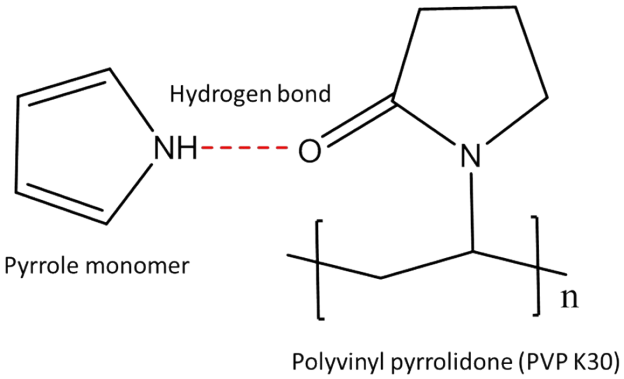

Fig.S2 Schematic diagram of pyrrole monomer adsorbed to the ketone group of PVP by a hydrogen bond.

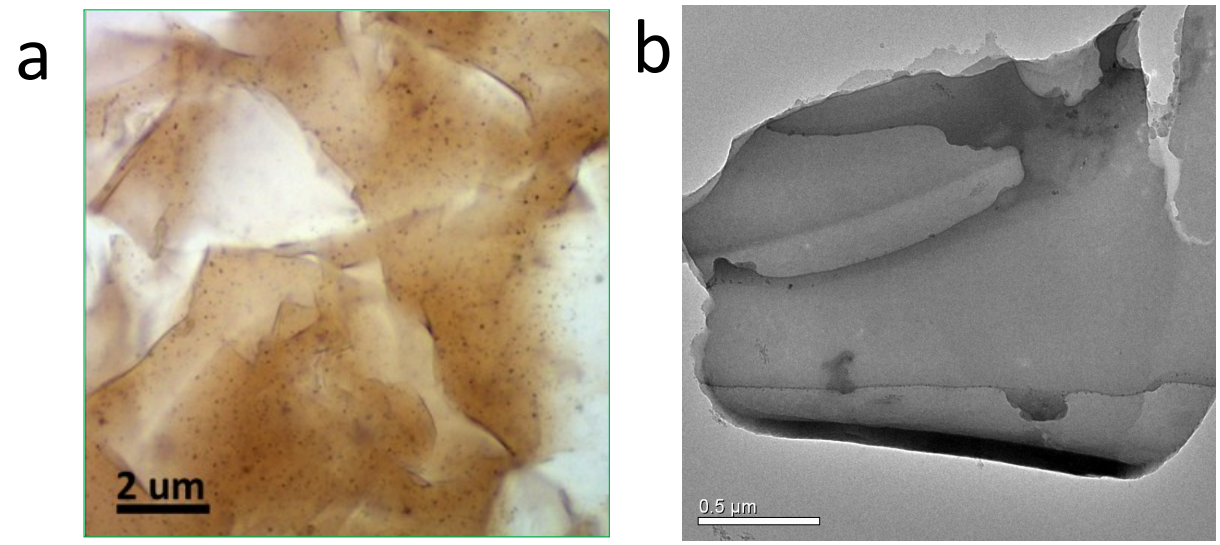

Fig.S3 (a) Optical image of polypyrrole nanosheets prepared by using ammonium persulphate as the polymerization initiator instead of $FeCl_3$. (b) The corresponding carbon sheets derived from the carbonization of polypyrrole nano-sheets at 800℃.

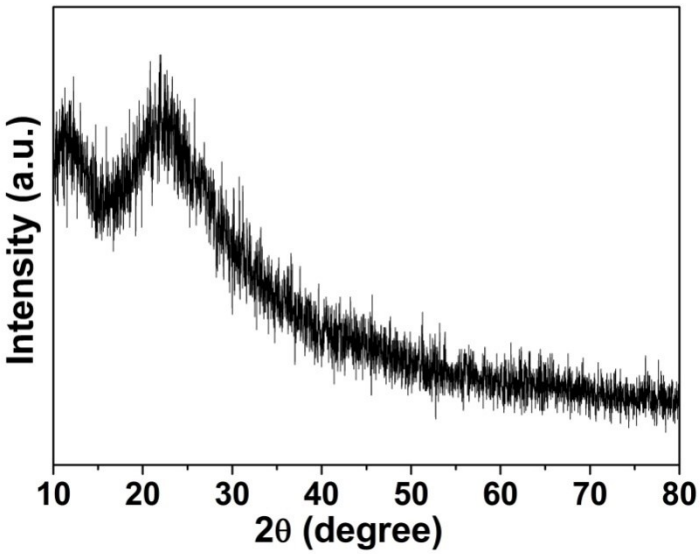

Fig.S4 Typical XRD pattern of PPyNSs. The diffraction peaks at 2θ of 12° and 23° are ascribed to crystalline polypyrrole.

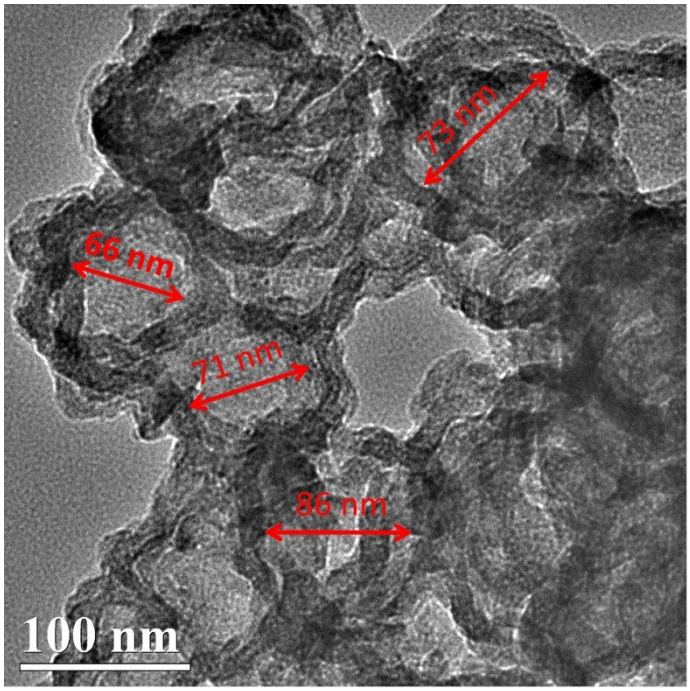

Fig.S5 Representative TEM image of HPC-800 with apparent macropores of 50-100nm.

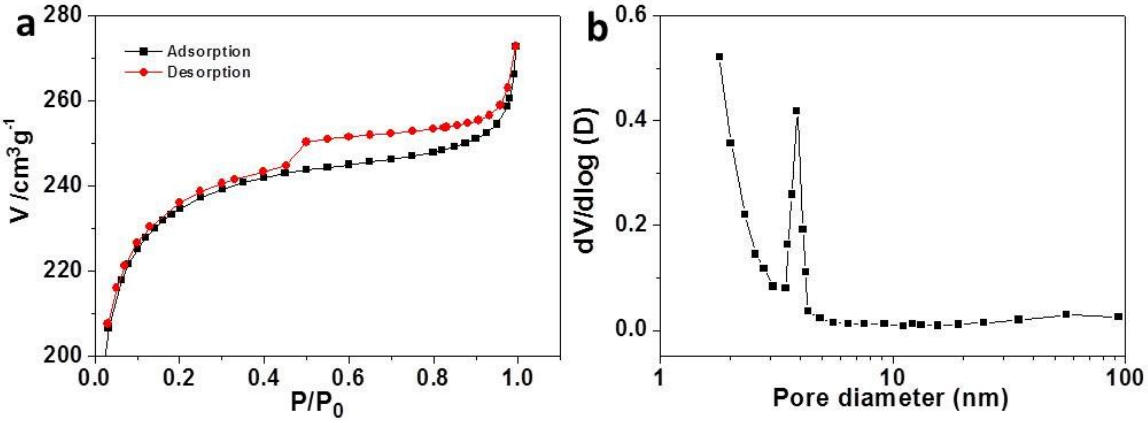

Fig. S6 (a) N_2 adsorption/desorption isotherm and (b) the corresponding pore size distribution of HPC-800.

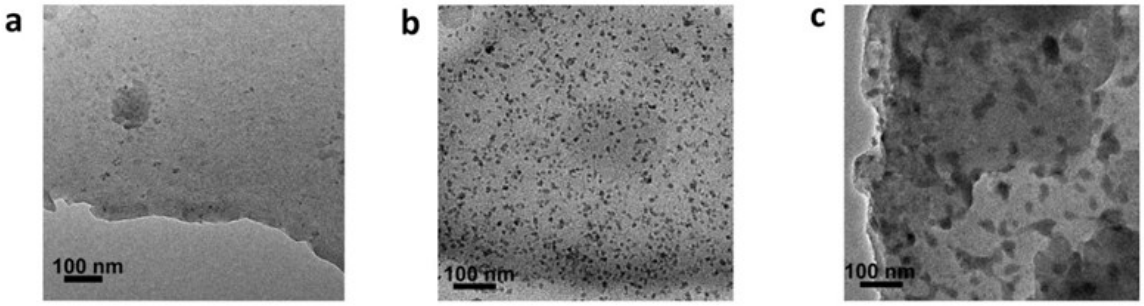

Fig. S7 RepresentativeTEM images of (a) PPyNSs, (b) HPC-300, and (c) HPC-500.

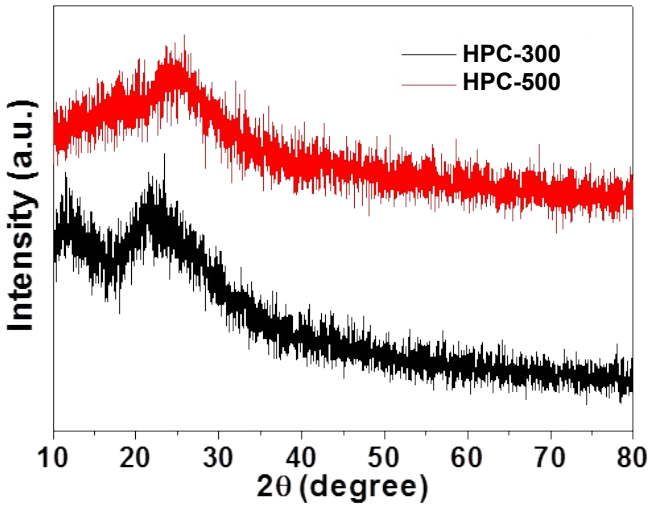

Fig. S8 XRD patterns of HPC-300 and HPC-500.

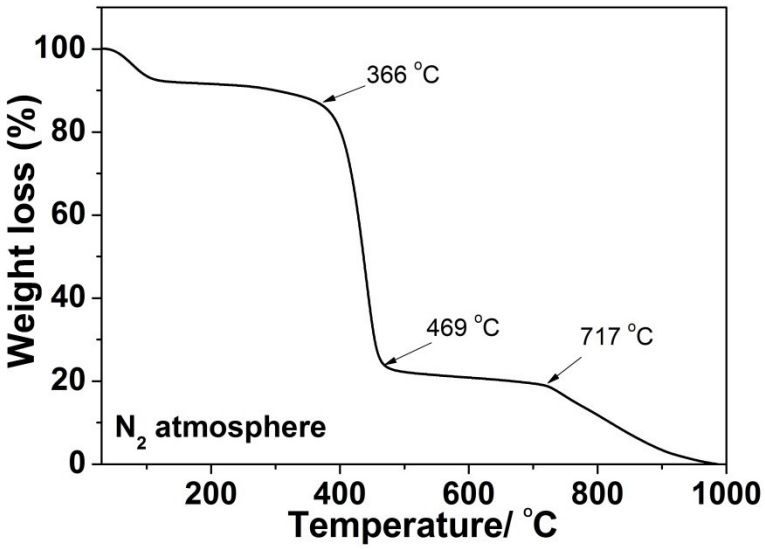

Fig. S9 TGA curve of PPyNSs from 30 to 1000°C in a N_2 atmosphere at a heating rate of 5°Cmin^{-1}.

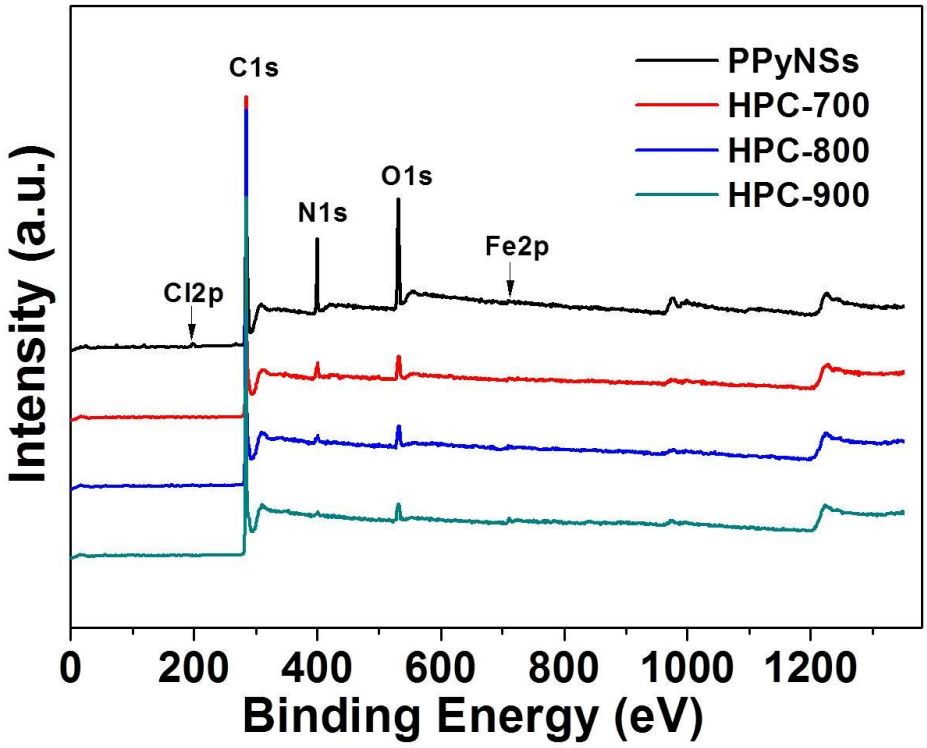

Fig. S10 XPS survey spectra of PPyNSs and HPC-T (T = 700, 800 and 900).

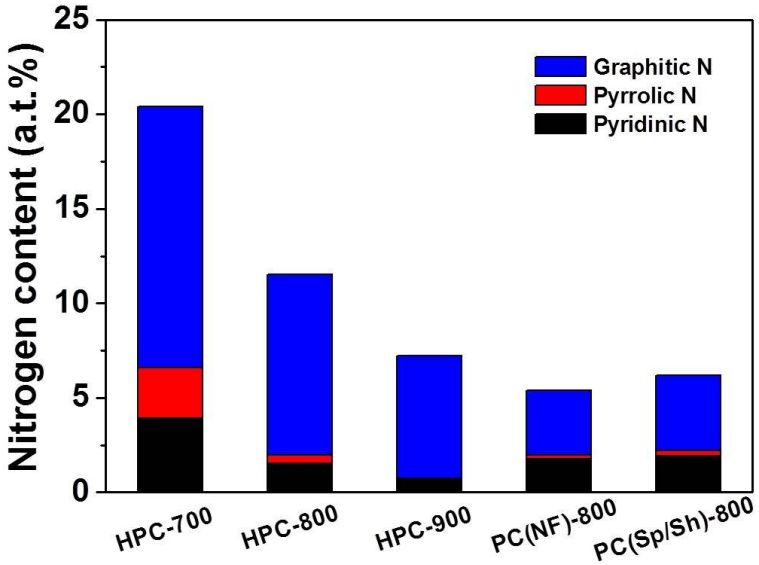

Fig. S11 Concentrations of graphitic N, pyrrolic N and pyridinic N in HPC-T (700, 800 and 900), PC(NF)-800 and PC(Sp/Sh)-800.

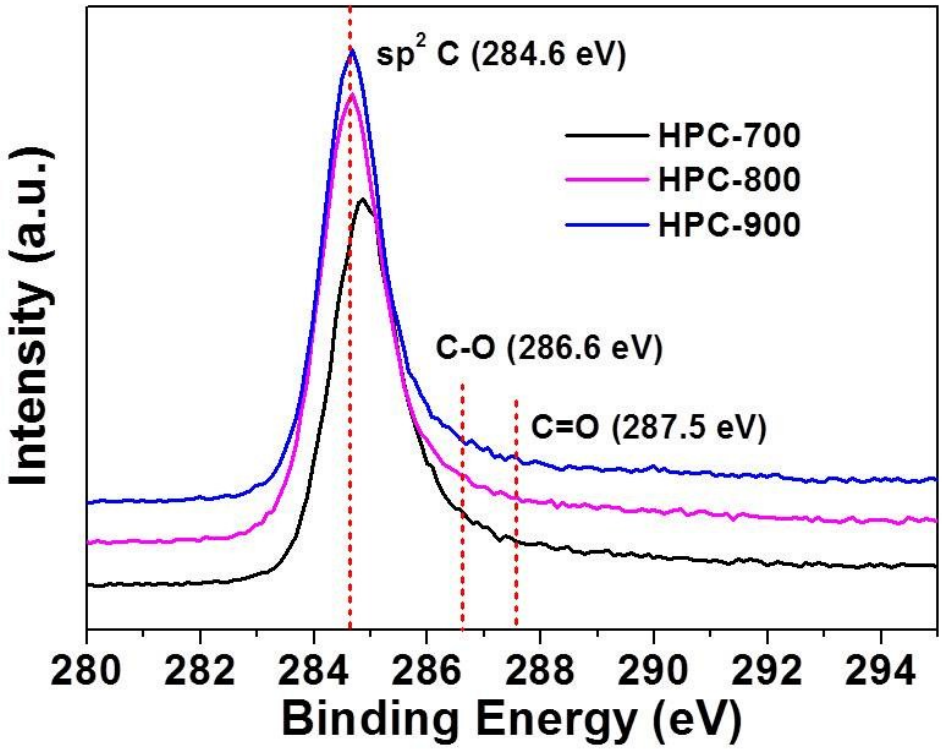

Fig. S12 C1s spectra of HPC-T (T=700, 800 and 900).

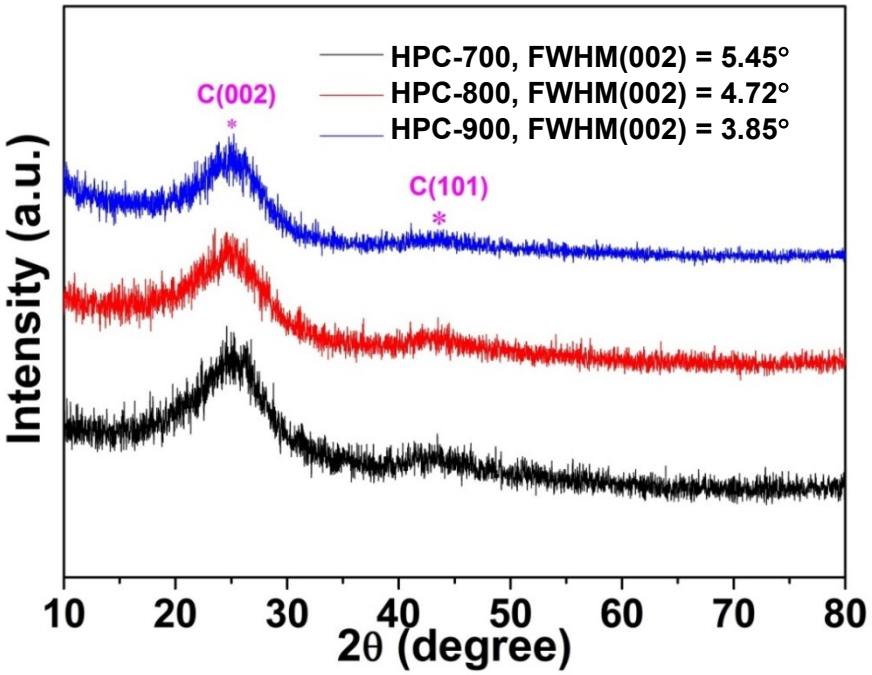

Fig. S13 XRD patterns of HPC-T (T=700, 800 and 900℃). One can see that with increasing pyrolysis temperature, the FWHM of the HPC-T (002) diffraction peaks decreased, indicating an increasing degree of graphitization in the sample.

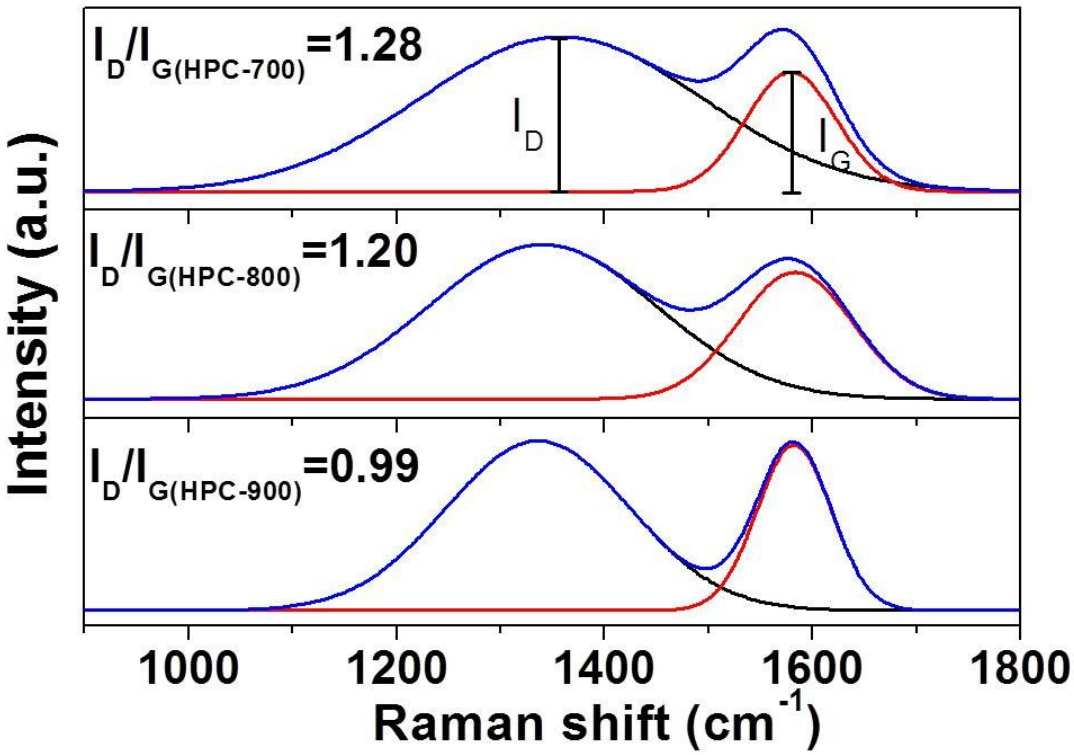

Fig.S14 Raman spectra of HPC-T (T = 700, 800 and 900). The graphitic D and G bands can be clearly seen at ca. 1354 cm^{-1} and 1578 cm^{-1}, respectively for all samples, and the intensity ratio of the D and G band (I_D/I_G) varied slightly with the pyrolysis temperature, which was observed at 0.94 for HPC-700, 0.97 for HPC-800 and 1.04 for HPC-900. That is, when the pyrolysis temperature was increased from 700 to 900 °C, one observed increasing graphitization of the sp^2 carbon walls in the macro/mesoporous carbon.

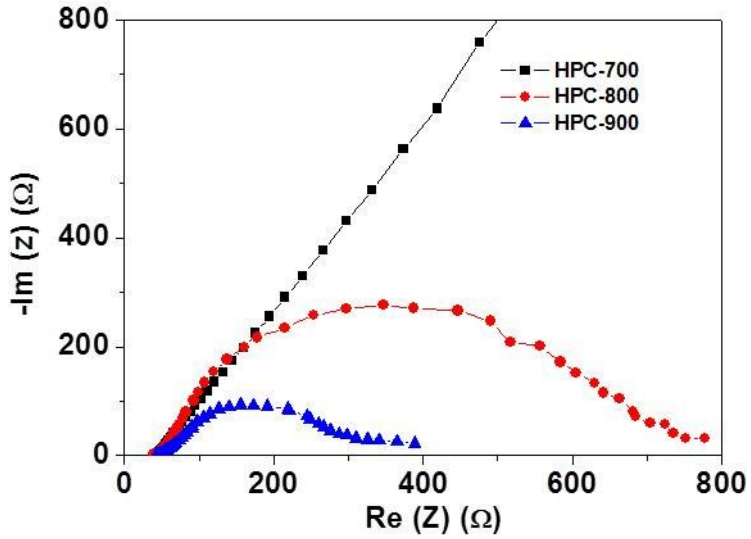

Fig.S15 Electrochemical impedance spectroscopy (EIS) spectra of HPC-T (T = 700, 800 and 900).The electrochemical impedance data was recorded in O_2-saturated 0.1 M KOH at +0.85 V vs RHE with an AC amplitude of 5 mV in frequency of 10 kHz to 0.01 Hz. Electrode rotation speed was 1600 rpm.

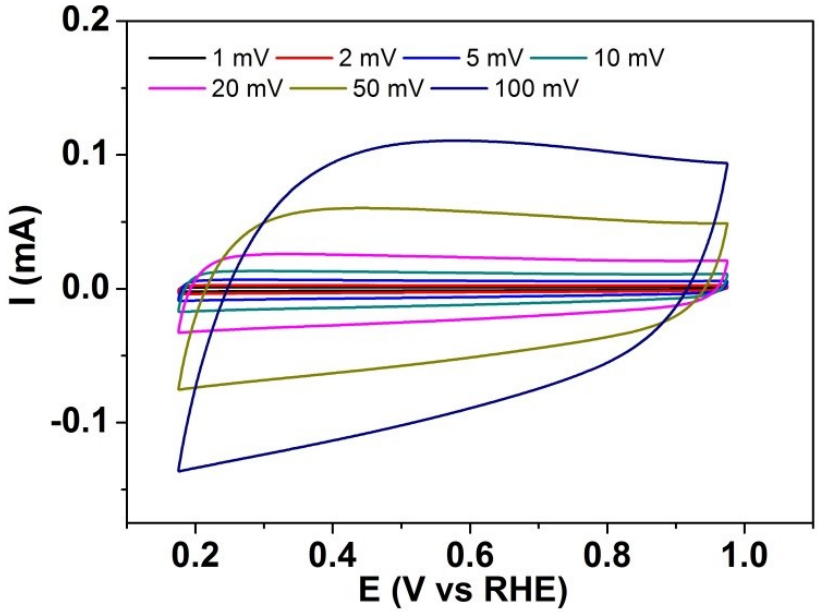

Fig.S16 CVs of HPC-800 in a N_2-saturated 6 M KOH aqueous solution at a sweep rate of $1mVs^{-1}$ to $100mVs^{-1}$.

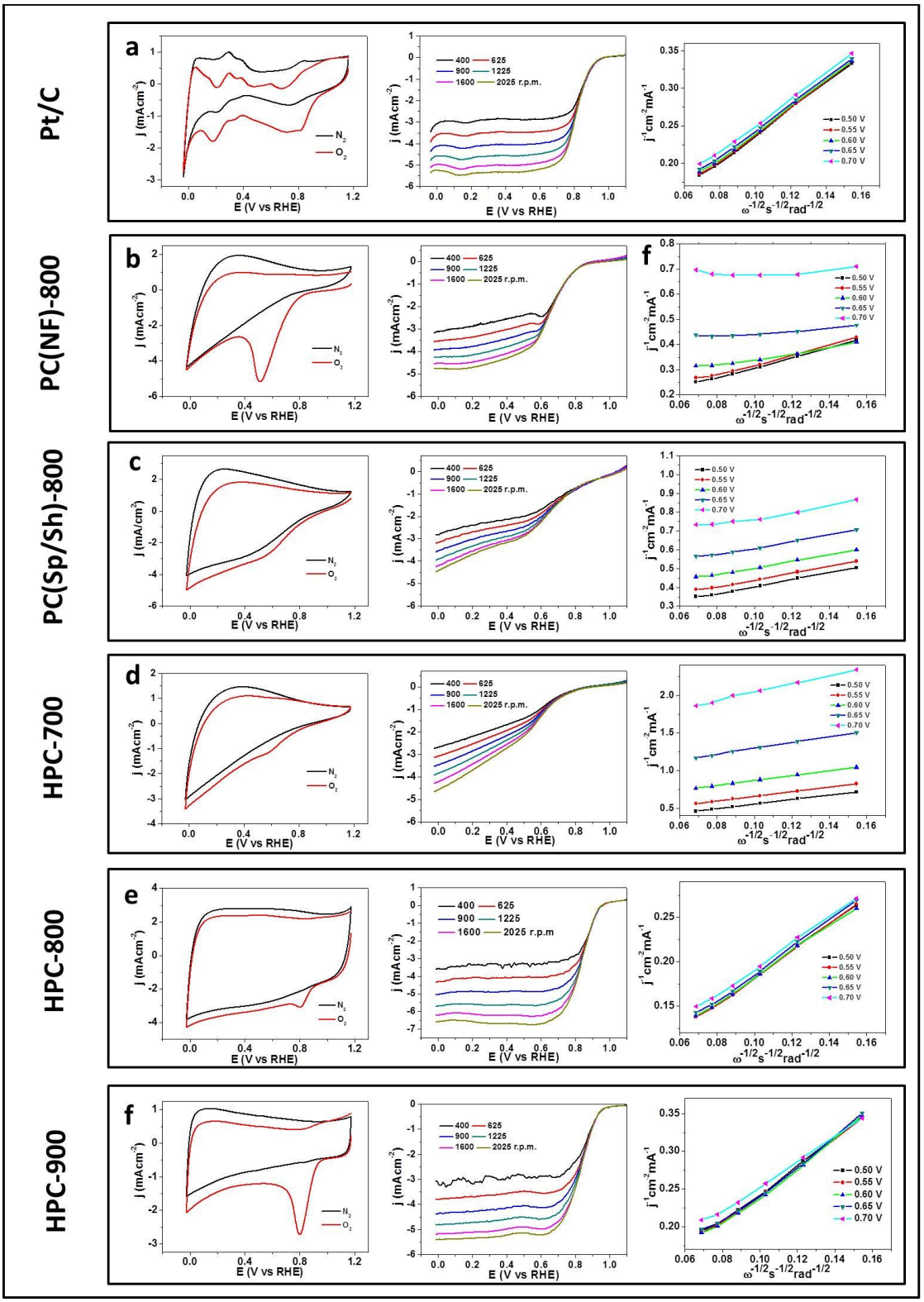

Fig.S17 CVs, RRDE curves and K-L plots of (a) Pt/C, (b) PC(NF)-800, (c) PC(Sp/Sh)-800, (d) HPC-700, (e) HPC-800 and (f) HPC-900 in O_2-saturated 0.1 M KOH at a potential sweep rate of 10 mVs^{-1} and electrode-rotation speed of 400 to 2025 rpm.

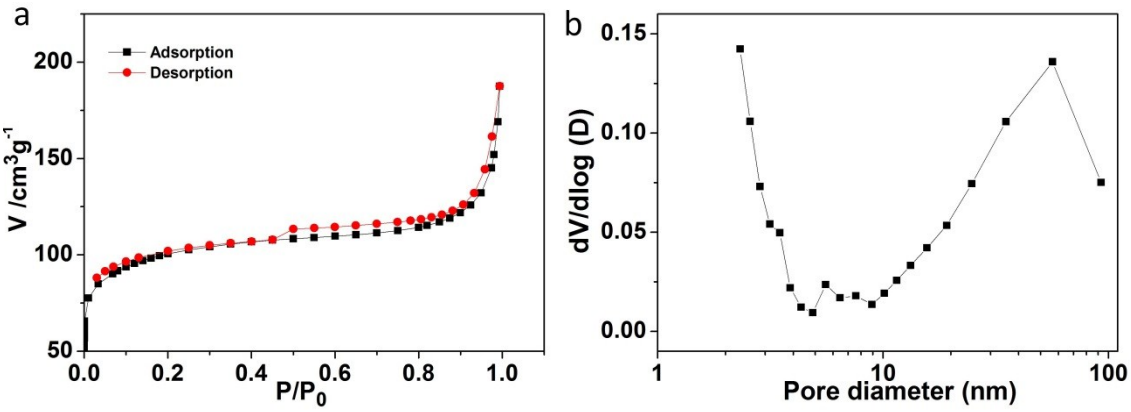

Fig.S18 (a) N_2 adsorption/desorption isotherm and (b) the corresponding pore size distribution of PC(NF)-800. The BET surface area of PC(NF)-800 was determined to be 345.9 m^2g^{-1}.The pore size distribution suggests that the PC(NF)-800 was composed of two kinds of pores, the small pores with a diameter size less than 4 nm, and the large pores with diameter in the range from 10 to 100 nm.

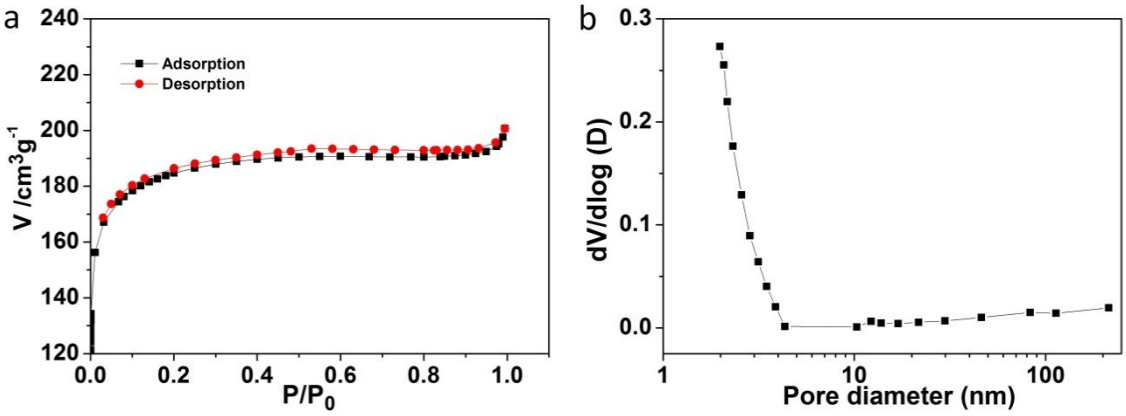

Fig.S19 (a) N_2 adsorption/desorption isotherm and (b) the corresponding pore size distribution of PC(Sp/Sh)-800 (BET surface area= 623.4 m^2g^{-1}, pore diameter< 3nm). The pore size distribution suggests that there was onlyone type of porous structure with a diameter less than 3 nm in PC(Sp/Sh)-800.

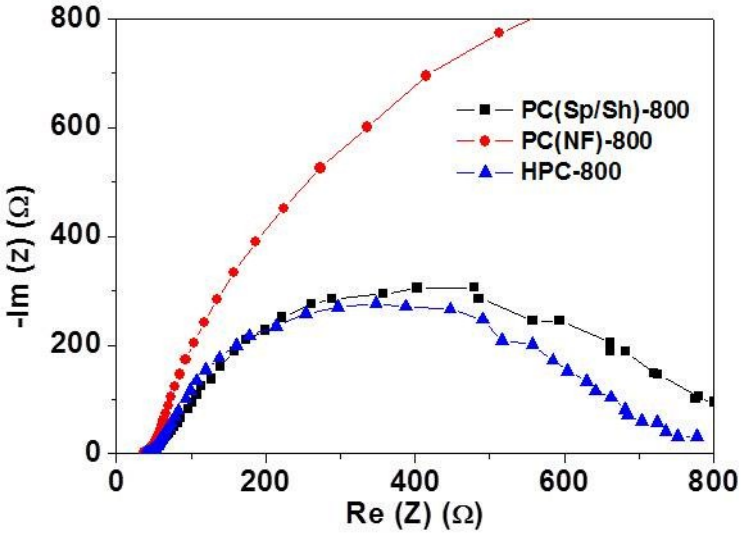

Fig.S20 Electrochemical impedance spectra of carbon catalysts derived from polypyrrole of different morphologies. The electrochemical impedance data was recorded in O_2-saturated 0.1 M KOH at +0.85 Vvs RHE with an AC amplitude of 5 mV in frequency of 10 kHz to 0.01 Hz. Electrode rotation speed was 1600 rpm.

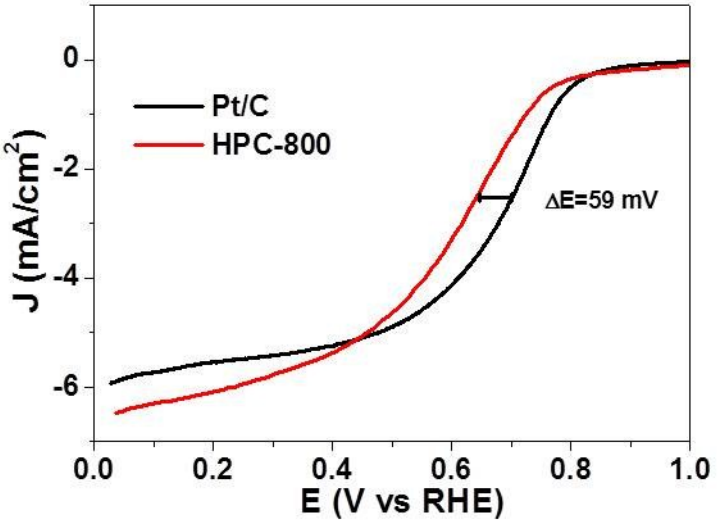

Fig.S21 LSV curves of HPC-800 and Pt/C in an O_2-saturated 0.1 M $HClO_4$ aqueous solution at a potential sweep rate of 10 mVs^{-1} with the electrode rotation speed of 1600 rpm.

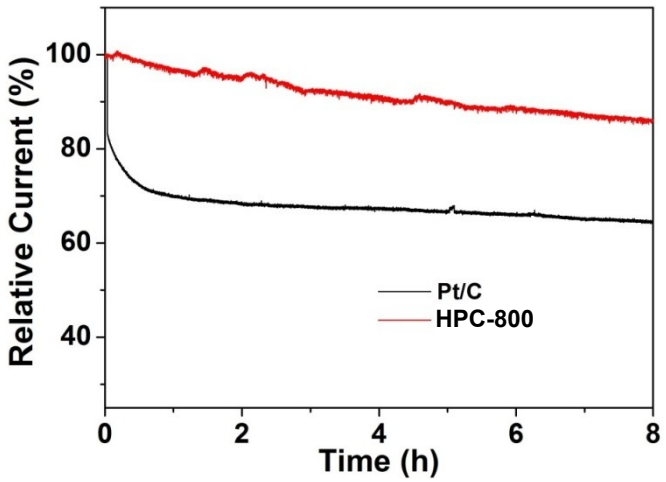

Fig.S22 Chronoamperometric curves of a glassy-carbon electrode modified with indicated catalysts at +0.60 V vs RHE in an O_2-saturated 0.1 M KOH solution. Electrode rotation speed was 1225 rpm.

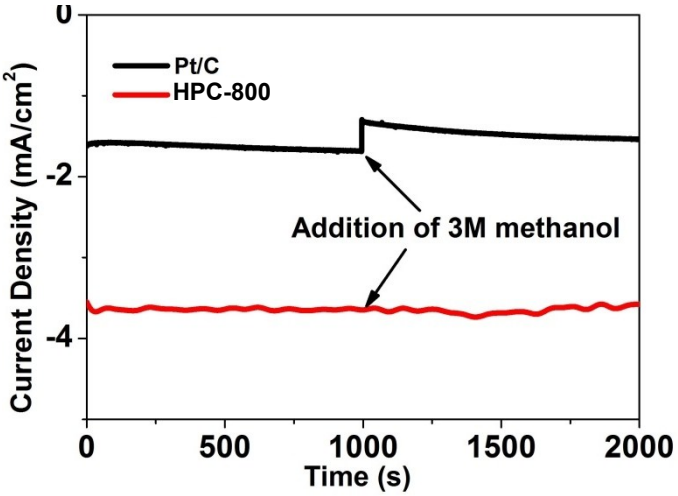

Fig.S23 Chronoamperometric curves of a glassy-carbon electrode modified with catalysts at +0.60 V vs RHE in an O_2-saturated 0.1 M KOH solution with 3 M methanol addition at 1000s. Electrode rotation speed 1225 rpm.

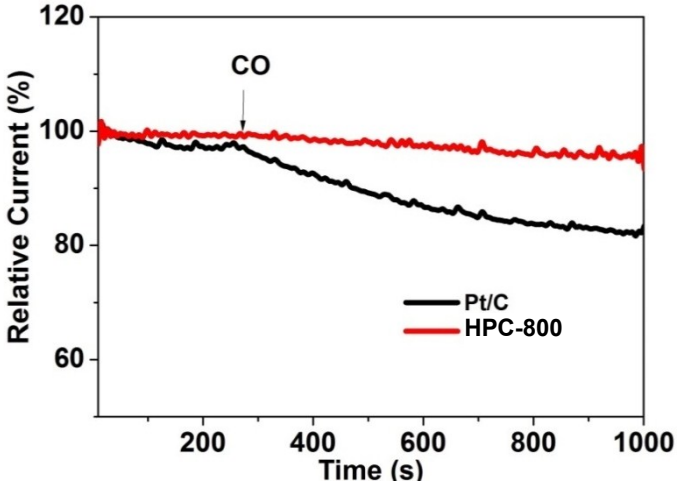

Fig.S24 Chronoamperometric curves of a glassy-carbon electrode modified with catalysts at +0.60 V vs RHE in an O_2-saturated 0.1 M KOH solution. CO was injected into the solution at 240s. Electrode rotation speed 1225 rpm.